

Charge-Dependent Correlations in Relativistic Heavy Ion Collisions and the Chiral Magnetic Effect

Adam Bzdak, Volker Koch, Jinfeng Liao

Abstract We provide a phenomenological analysis of present experimental searches for local parity violation manifested through the Chiral Magnetic Effect. We introduce and discuss the relevant correlation functions used for the measurements. Our analysis of the available data from both RHIC and LHC shows that the present experimental evidence for the Chiral Magnetic Effect is rather ambiguous. We further discuss in some detail various background contributions due to conventional physics, which need to be understood quantitatively in order to draw a definitive conclusion about the existence of local parity violation in heavy ion collisions.

To appear in Lect. Notes Phys. "Strongly interacting matter in magnetic fields" (Springer), edited by D. Kharzeev, K. Landsteiner, A. Schmitt, H.-U. Yee

Adam Bzdak
RIKEN BNL Research Center, Brookhaven National Laboratory, Upton, NY 11973, USA.
e-mail: abzdak@bnl.gov

Volker Koch
Nuclear Science Division, Lawrence Berkeley National Laboratory, MS70R0319, 1 Cyclotron Road, Berkeley, California 94720, USA.
e-mail: vkoch@lbl.gov

Jinfeng Liao
Physics Department and Center for Exploration of Energy and Matter, Indiana University, 2401 N Milo B. Sampson Lane, Bloomington, IN 47408, USA.
RIKEN BNL Research Center, Brookhaven National Laboratory, Upton, NY 11973, USA.
e-mail: liaoji@indiana.edu

1 Introduction

The theoretical study of topological solitons in field theories has a long history. Quite generically, these objects arise as solutions to the classical equations of motion for field theories due to the nonlinearity of the equations as well as due to specific boundary conditions. They are found in field theories of various dimensions (2D kinks, 3D monopoles, 4D instantons), and are known to be particularly important in the non-perturbative domain where the theories are strongly coupled. For a recent review, see e.g. [1].

Topological objects in Quantum Chromodynamics (QCD) are known to play important roles in many fundamental aspects of QCD [1]. For example, instantons are responsible for various properties of the QCD vacuum, such as spontaneous breaking of chiral symmetry and the $U_A(1)$ anomaly (see e.g. [2, 3]). Magnetic monopoles, on the other hand, are speculated to be present in the QCD vacuum in a Bose-condensed form which then enforces the color confinement, known as the dual superconductor model for QCD confinement, which is strongly supported by lattice QCD calculations (see e.g. [4, 5]). Alternatively vortices are believed to describe the chromo-electric flux configuration (i.e. flux tube) between a quark-anti-quark pair in the QCD vacuum which in turn gives rise to the confining linear potential (see e.g. reviews in [5, 6]). Some of these objects, such as monopoles [7] and flux tubes [8], may also be important degrees of freedom in the hot and deconfined QCD matter close to the transition temperature T_c , and may be responsible for the observed properties of the so called strongly coupled quark-gluon plasma [9, 10].

Since the existence of such topological objects is theoretically well motivated and their effects on the dynamics are deemed to be important, a direct experimental detection of such objects or at least of certain unique imprints by them, would be a highly desirable goal. This review will discuss recent efforts and progress toward that goal, specifically in the context of relativistic heavy ion collisions through the measurement and analysis of charge-dependent correlations.

1.1 The Chiral Magnetic Effect in brief

An interesting suggestion by Kharzeev and collaborators [11, 12, 13, 14, 15, 16] on the direct manifestation of effects from topological objects is the possible occurrence of \mathcal{P} - and \mathcal{CP} -odd (local) domains due to the so-called sphaleron or anti-sphaleron transitions in the hot dense QCD matter created in relativistic heavy ion collisions. Imagine that in a single event created in a heavy ion collision the gauge field configurations in the space-time zone of the created hot dense matter experience a single sphaleron transition. As a result this local zone acquires a non-zero topological charge which is parity-odd.

This non-zero topological charge, when coupled with light quarks through the triangle anomaly, induces a non-zero chirality for the quarks. In other words it generates an imbalance between left- and right-handed quark numbers, or a non-zero axial charge density. To be precise, there is no violation of parity at the interaction level, but rather a local creation of matter with non-zero axial charge density, which is a \mathcal{P} - and \mathcal{CP} -odd quantity.

A concrete proposal for experimental detection is the so-called Chiral Magnetic Effect (CME) [13]. The effect itself states that in the presence of external electromagnetic (EM) magnetic field \mathbf{B} , a nonzero axial charge density will lead to an EM electric current along the direction of the magnetic field \mathbf{B} :

$$\mathbf{j}_V = \frac{N_c e}{2\pi^2} \mu_A \mathbf{B} \quad (1)$$

where μ_A is the axial chemical potential associated with the non-zero axial charge density present in the system, and N_c is the number of colors. This elegant relation is theoretically well established in both the weakly-coupled and the strongly-coupled regimes of the theory as will be discussed in several contributions to this volume.

At first sight, it might seem that the above relation is violating parity: under spatial rotation and inversion the EM electric current \mathbf{j}_V transforms like a vector, while the magnetic field, \mathbf{B} , transforms like an axial- or pseudo-vector. Therefore, the factor in Eq. (1) relating the two will have to be parity-odd. This is indeed the case, since μ_A that enters the above relation is a pseudo-scalar quantity which changes sign under parity transformation. Thus the CME relation, Eq. (1), is invariant under parity transformation. However, in a region with nonzero, either positive or negative, μ_A certain parity-odd observables, e.g. the pseudoscalar quantity $\langle \mathbf{j}_V \cdot \mathbf{B} \rangle$, may acquire nonzero expectation values. It is only in this sense that one may refer to it as “local parity violation”.

In addition there is a complimentary relation, as one might have guessed from the “duality” by interchanging the roles of V (vector) and A (axial), that has been called the Chiral Separation Effect (CSE). The CSE refers to the separation of chiral (or axial) charge along the axis of the external EM magnetic field at finite density of the vector charge, for example at finite baryon number density [17, 18]. The resulting axial current is given by

$$\mathbf{j}_A = \frac{N_c e}{2\pi^2} \mu_V \mathbf{B} \quad (2)$$

with the μ_V here being the baryon number chemical potential. Furthermore the combination of the two effects, CME and CSE, gives rise to an interesting propagating collective mode: the vector density induces an axial current which transports and creates a locally nonzero axial charge density, which in turn leads to a vector current that further transports and creates a locally nonzero vector density, and so on. This is called Chiral Magnetic Wave

(CMW) [19], just like Maxwell's electromagnetic waves represent the coupled evolution of the electric and magnetic fields. The CMW is a general concept that includes both the CME and CSE effects. It is robust in the sense that it takes the form of a collective excitation like the sound wave without relying on a quasi-particle picture.

We end the general introduction with two comments: first, the CME in the language of CMW induces a charged dipole (of the vector density distribution) that results from an initial nonzero axial charge density; second it has been recently pointed [20] that an initial vector charge density via CMW will lead to a charged quadrupole distribution that may be observable in heavy ion collisions. For the rest of this contribution we will focus on the charged dipole signal for the CME phenomenon.

1.2 Hunting for the CME in heavy ion collisions

Now we turn to two key questions: can the Chiral Magnetic Effect occur in heavy ion collisions, and if so, what observables serve as unambiguous signals for the CME?

The answer to the first question seems to be positive. Two elements are needed for the CME to occur: an external magnetic field and a locally nonzero axial charge density. The relativistically moving heavy ions, typically with large positive charges (e.g. $+79e$ for Au), carry strong magnetic (and electric) fields with them. In the short moments before/during/after the impact of two ions in non-central collisions, there is a very strong magnetic field in the reaction zone [21, 13]. In fact, such a magnetic field is estimated to be of the order of $m_\pi^2 \approx 10^{18}$ Gauss [22, 23] (see also [24]), probably the strongest, albeit transient, magnetic field in the present Universe. The other required element, a locally non-vanishing axial charge density, can also be created in the reaction zone during the collision process through sphaleron transitions (see e.g. [16] for discussions and references therein). As such, it appears at least during the very early stage of a heavy ion collision, there can be both strong magnetic field and nonzero axial charge density in the created hot matter. Therefore, the CME should take place, that is, an electric current will be generated either parallel or anti-parallel to the magnetic field \mathbf{B} depending on the axial charge density is positive (due to sphaleron) or negative (due to anti-sphaleron). How large this current is, is of course another question, see e.g. [25].

The answer to the second question is much more difficult. Extracting the effects of the CME, which most likely occur at the very early stage of the collision, from the final observed hadrons, involves many uncertainties. First, it is quite unclear how long the magnetic field could remain strong: while the peak value is large, it decays very rapidly with time (if the only source of such field is from the protons in the ions) [26]. Second, if the CME current

is generated mostly at very early time, it is not clear to which extent this current could survive without significant modifications, since we know that the created quark-gluon plasma behaves like a strongly interacting fluid. Furthermore, even if this current survives, one has to find the right observable for its detection. At present, there is no satisfactory resolution on the first two issues. This will likely require comprehensive and quantitative model studies. In this review we will only focus on the third issue — the observables to be used for measuring the possible CME current and related “background” effects.

In a simplistic view, one may consider the ultimate manifestation of the CME as a separation of charged hadrons along the direction of the initial magnetic field: more positive hadrons moving in one direction while more negative hadrons in the opposite direction. As a result, the momentum distribution of the final hadrons will have a charged dipole moment. The direction of such a momentum space dipole is expected to be along the \mathbf{B} field, parallel or anti-parallel, depending on the sign of the initial axial charge density in a given event. Since the initial axial charge may be positive and negative with equal probability, the event average of the momentum space dipole vanishes, $\langle \mathbf{j}_V \cdot \mathbf{B} \rangle = 0$. This reflects the fact that parity is not broken globally by the strong interaction, so that any pseudo-scalar quantity, such as $\langle \mathbf{j}_V \cdot \mathbf{B} \rangle$, will have to vanish. What one can hope for, however, is to measure the fluctuation or variance of this charge separation, i.e. $\langle (\mathbf{j}_V \cdot \mathbf{B})^2 \rangle$, which is a parity even quantity. As we will discuss later, the prize one has to pay is that other, conventional correlations, not related to the CME, may contribute to observables which are sensitive to the variance of charged dipole moment.

Recently the STAR collaboration at the Brookhaven’s Relativistic Heavy Ion Collider (RHIC) has reported [27] first measurements of a charge dependent correlation function in heavy ion collisions, which may be sensitive to the Chiral Magnetic Effect. The essential idea of the measurement, proposed by Voloshin [28], is based on two important features: first, in non-central heavy ion collisions, the direction of initial strong magnetic field is strongly correlated with the so-called reaction plane, which is spanned by the impact parameter and the beam direction. The \mathbf{B} field is pointing (mostly) along the normal of reaction plane, albeit with random up/down orientation; second, the CME-induced current, or the charged dipole in momentum space, implies particular charge-dependent correlation patterns. The same-sign charged hadrons will prefer moving together while the opposite-sign charged hadrons moving back-to-back along the \mathbf{B} field direction, and thus perpendicular to the reaction plane, which is commonly referred to as the out-of-plane direction ¹. While these measurements and their implications will be discussed in detail in Section 3, let us briefly summarize the present

¹ As a note of caution, the strong correlation between the \mathbf{B} field direction and the participant-plane are considerably modified when the strong fluctuations in the initial condition are properly taken into account. As a result the two are rather weakly correlated in very central and very peripheral collisions [23, 24, 29].

status: the STAR (later PHENIX, and also ALICE) data show very interesting charge dependent azimuthal correlation patterns, and some features are in line with the CME predictions. Other aspects of the data, on the other hand, are very hard to understand within the framework of the CME. At present, therefore, the observation of the Chiral Magnetic Effect in heavy ion collisions, and the local parity violation in the aforementioned sense, has not been established experimentally, and additional measurements as well as further theoretical analysis are required before definitive conclusions can be drawn.

This review is organized as follows: in Section 2, we will present a general discussion on the charge-dependent correlation measurements in heavy ion collisions, with the emphasis on the CME related observables; in Section 3, the presently available data from heavy ion collisions at a variety of collision energies will be examined and their interpretations will be critically evaluated; in Section 4, various possible “background” effects and their manifestation in various observables will be quantitatively analyzed; finally in Section 5 we summarize and conclude.

2 The charge-dependent correlation measurements

In this Section, we focus on various charge-dependent correlation measurements in heavy ion collisions and what can be learned from these observables. The emphasis will not be on the data themselves, which will be the subject of the next Section. Instead we will set up the conceptual framework for studying the azimuthal correlations, discuss possible complications in the design of the observables, and examine the connection between physical effects and the measurements.

2.1 General considerations concerning azimuthal correlation measurements

The basic experimental information about the (hadronic) final state of a heavy ion collision consists of the momenta and the identity – the electric charge, mass and possibly other quantum numbers – of all hadrons observed in the acceptance of a given experiment. Customarily, the three-momentum \mathbf{p} is represented by the (longitudinal) rapidity, y , the transverse momentum p_t as well as the azimuthal angle ϕ . Events may further be grouped according to the charged particle multiplicity, which is a good measure of the centrality or impact parameter of a collision. From a given sample of events one can then extract the single particle distributions, $d^3N/dydp_t^2d\phi$ either

for all charged hadrons or, more selectively, for identified pions, kaons, protons, etc. In order to study possible correlations one analyses two-particle, three-particle and multi-particle distributions of various kinds. Most of the discussion in this review will focus on the dependence of various measurements on the azimuthal angle. The rapidity y and the transverse momentum p_t will either be in specific bins or integrated over.

The analysis of azimuthal distributions has to deal with the fact that the azimuthal direction of each collision, characterized by either the direction of the angular momentum or the impact parameter, is randomly distributed in the laboratory frame. Therefore, a single particle azimuthal distribution, $dN/d\phi$ will always be uniform and, thus, rather meaningless. To learn something about azimuthal distributions, one either measures distributions of the difference of the azimuthal angles of two particles, $dN/d(\phi_1 - \phi_2)$, or one determines the azimuthal orientation of a given event and studies distributions with respect to this direction. Commonly the azimuthal direction of the so-called reaction plane is used to characterize the orientation of an event. As already discussed in the Introduction, the reaction plane is spanned by the beam direction and the impact parameter of the collision. Its orientation in the laboratory frame is given by the so-called reaction plane angle, Ψ_{RP} , which measures the direction of the impact parameter in the laboratory frame. Given the reaction plane angle, one then can study azimuthal angular distributions with respect to the reaction plane angle, $f(\phi - \Psi_{RP}) = dN/d(\phi - \Psi_{RP})$. Clearly the determination of the reaction plane requires the measurement of other particles in addition to that used for the angular distribution (for a comprehensive review, see [30]). Therefore, the extraction of azimuthal distributions will require the measurement of two-particle (for the angular difference distribution $dN/d(\phi_1 - \phi_2)$) or even higher particle distributions.

However, it is important to distinguish between the need to measure two- or many-particle distributions to study azimuthal distributions, and the presence of true dynamical two- or many- particle correlations. To make this distinction more transparent, it is useful to introduce an *intrinsic* frame or coordinate system where the x -direction is given by the direction of the impact parameter, which is typically referred to as the so-called “in-plane-direction”, and the y direction is defined by the angular momentum, or the so-called “out-of plane direction”. The relative angle of the x -axis of the intrinsic frame and that of the laboratory frame is then given by the reaction plane angle Ψ_{RP} , as illustrated in Fig.1. In theoretical considerations and model calculations the orientation of the reaction plane is assumed to be known, or in other words, these calculations take place in the intrinsic frame. Finally, the azimuthal angle Φ in the intrinsic frame is related to the laboratory angle ϕ by

$$\Phi = \phi - \Psi_{RP} \quad (3)$$

To continue, let us, as an example, consider a single particle distribution in the intrinsic frame

$$f_1(\Phi) = f_1(\phi - \Psi_{RP}) \propto 1 + 2v_2 \cos[2(\Phi)] = 1 + 2v_2 \cos[2(\phi - \Psi_{RP})] \quad (4)$$

which has an azimuthal asymmetry, characterized by the second Fourier component of strength v_2 . This kind of distribution, which will be relevant for the subsequent discussion, is important in the context of the observed azimuthal asymmetries in heavy ion collisions, which are generally attributed to the hydrodynamics evolution of the system in non-central collisions. The parameter v_2 is commonly referred to as the elliptic flow coefficient. For a detailed discussion see [30]. The value for the elliptic flow parameter, v_2 , may be obtained by measuring the second moment of the angular distribution, $\langle \cos 2(\phi - \Psi_{RP}) \rangle$. To this end we have to determine the reaction plane angle in each event, calculate the average moment in the intrinsic frame of each event and then average over events:

$$\begin{aligned} & \langle \cos [2(\phi - \Psi_{RP})] \rangle \\ &= \frac{1}{N_{\text{events}}} \sum_{\text{event } i=1}^{N_{\text{events}}} \left\{ \frac{1}{N(i)} \sum_{\text{particle } k=1}^{N(i)} \cos [2(\phi_k - \Psi_{RP}(i))] \right\} \end{aligned} \quad (5)$$

In terms of the distribution function f_1 this can be expressed as²

$$\langle \cos [2(\phi - \Psi_{RP})] \rangle = \frac{\int d\Psi_{RP} \int d\phi f_1(\phi - \Psi_{RP}) \cos [2(\phi - \Psi_{RP})]}{\int d\Psi_{RP} \int d\phi f_1(\phi - \Psi_{RP})} \quad (6)$$

Let us next consider the two-particle distribution

$$f_2(\Phi_1, \Phi_2) = f_1(\Phi_1)f_1(\Phi_2) + C(\Phi_1, \Phi_2) \quad (7)$$

where the first term is simply the product of the single particle distributions, and the second term, $C(\Phi_1, \Phi_2)$ represents possible, *true*, two-particle correlations. Since the two-particle distribution depends on two angles, Φ_1 and Φ_2 , in general it will have terms which depend only on the difference of the angle $\sim (\Phi_1 - \Phi_2) = (\phi_1 - \phi_2)$, and which are independent of the direction of the reaction plane. It will also have terms which depend on the sum of the angles, $\sim (\Phi_1 + \Phi_2) = (\phi_1 + \phi_2 - 2\Psi_{RP})$ which are dependent on the reaction plane direction. This may be illustrated by inserting into Eq. (7) the single particle distribution, Eq. (4), and neglecting the correlation term, i.e., setting $C(\Phi_1, \Phi_2) = 0$. In this case

² In reality the ability to express the actual measurement, as described in Eq. (5), in terms of an average of moments of the intrinsic distribution over the reaction plane angle requires a detailed analysis of all non-flow effects and flow fluctuations, as discussed in detail in Ref. [30].

$$\begin{aligned}
f_2(\Phi_1, \Phi_2) &= f_1(\Phi_1)f_1(\Phi_2) \\
&\sim 2v_2^2 \cos[2(\Phi_1 - \Phi_2)] + 2v_2^2 \cos[2(\Phi_1 + \Phi_2)] \\
&= 2v_2^2 \cos[2(\phi_1 - \phi_2)] + 2v_2^2 \cos[2(\phi_1 + \phi_2 - 2\Psi_{RP})] \quad (8)
\end{aligned}$$

The term $\sim \cos[2(\phi_1 - \phi_2)]$ which depends on the difference of the angles can then be extracted by the measurement of the two-particle correlation

$$\langle \cos[2(\phi_1 - \phi_2)] \rangle \sim \int_{\Phi_1} \int_{\Phi_2} f_2(\Phi_1, \Phi_2) \cos[2(\phi_1 - \phi_2)] \quad (9)$$

The measurement of the term $\sim \cos[2(\phi_1 + \phi_2 - 2\Psi_{RP})]$ requires the determination of the reaction plane, or at least a three-particle correlation measurement. For our example, Eq. (8), $\langle \cos[2(\phi_1 - \phi_2)] \rangle \sim v_2^2$, and in fact this is one of the frequently used (and the simplest) methods for measuring the elliptic flow. However, this method suffers from the so-called “non-flow” [30] contributions, which are due to the correlation term we have neglected in our example. Our simple example also demonstrates a very important fact: single particle distributions, such as f_1 do contribute to multi-particle azimuthal correlations. This will be essential for the subsequent discussion where one of the tasks will be to disentangle the effects from true correlations and contributions from the single particle distributions.

The above discussion can be easily extended to three- (and more) particle densities with the same basic conclusions:

- The n-particle density will have terms which do not depend on the reaction plane, and thus may be extracted by the measurement of appropriate n-particle correlations. It will also have reaction plane dependent terms,

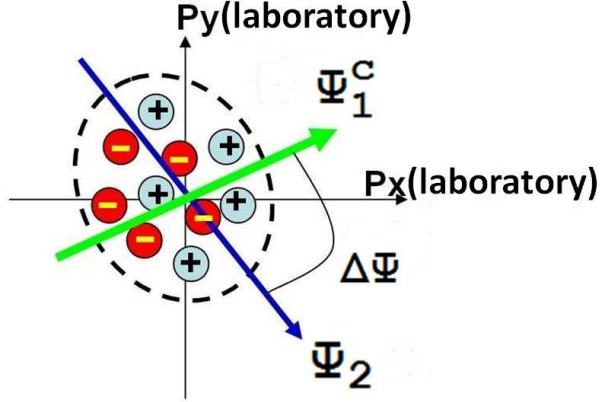


Fig. 1 A schematic demonstration of the proposed simultaneous analysis of \hat{Q}_1^c and \hat{Q}_2 vectors in the same event.

which require the measurement of at least $n+1$ particle correlations or the determination of the reaction plane.

- Unless not very carefully designed, multi-particle correlations will contain contributions from the single particle distribution.

Finally, the measurement of angular correlations is of course not restricted to the second Fourier moment. Recently the harmonic moments, $\langle \cos[n(\phi_1 - \phi_2)] \rangle$, have been measured in order to study flow fluctuations [31]. These correlations may also be measured in a more selective way, such as correlations for particles with same or opposite electric charges (the charge-dependent correlations), correlations for particles with certain quantum numbers (e.g. baryon-strangeness [32]), or correlations for particles within or between certain kinematic regions (e.g. the soft-hard correlations [33]), etc.

2.2 *Measuring the charge separation through azimuthal correlations*

Let us turn to possible azimuthal correlation measurements as the signal for the Chiral Magnetic Effect. Specifically, as discussed in the Introduction, we have to find azimuthal correlations which are sensitive to a possible out-of-plane “charge separation”.

We begin by defining what we mean by “charge separation effect”. Consider the distribution of final state hadrons in the transverse momentum space as schematically shown in the Fig. 1. If the “center” of the positive charges happens to be different from that of the negative charges, then there is a separation between two types of charges which may be quantified by an “electric dipole moment” in the transverse momentum space. Such a separation may arise either simply from statistical fluctuations or may be due to specific dynamical effect such as the CME. We note that such a charge separation occurs already at the single-particle distribution level in the *intrinsic* frame. Let us, therefore, define a charge-dependent single-particle azimuthal distribution, which, besides a possible momentum-space electric dipole moment, also includes the presence of elliptic flow:

$$f_\chi(\phi, q) \propto 1 + 2v_2 \cos[2(\phi - \Psi_{RP})] + 2q\chi d_1 \cos(\phi - \Psi_{CS}) \quad (10)$$

Here q and ϕ represent the charge and the azimuthal angle of a particle, respectively. The parameters v_2 and d_1 quantify the elliptic flow and the charge separation effect, while Ψ_{CS} specifies the azimuthal orientation of the electric-dipole and Ψ_{RP} the direction of the reaction plane (see Fig. 1). It is important to notice that an additional random variable $\chi = \pm 1$ is introduced. This accounts for the fact that in a given event we may have sphaleron or anti-sphaleron transitions resulting in charge separation parallel or anti-parallel to the magnetic field. Consequently the sampling over all events with a given

reaction plane angle, Ψ_{RP} , corresponds to averaging the intrinsic distribution f_χ over χ , namely $f_1 = \langle f_\chi \rangle_\chi \propto 1 + 2v_2 \cos(2\phi - 2\Psi_{RP})$. Physically speaking this means that the charge separation (or electric dipole, being \mathcal{P} -odd) flips sign randomly and averages to zero, thus causing the expectation value of any parity-odd operator to vanish. However, since $\langle \chi^2 \rangle = 1$ the presence of an event-by-event electric dipole may be observable through its variance.

For measurements related to heavy ion collisions one may reasonably assume particle charges to be $|q| = 1$ which is the case for almost all charged particles, e.g., charged pions and kaons, protons, etc. We note, that the above distribution does *not* contain a directed flow term $\sim \cos(\phi - \Psi_{RP})$ for either type of charges, which is reasonable if the distribution is measured in a symmetric rapidity bin.

Finally one may also consider a p_t -differential formulation of the charge separation effect or charge separation effects associated with higher harmonics in the azimuthal angle ϕ . We note that the charge separation term considered in Eq. (10) is actually the lowest harmonic in a more general charge-dependent Fourier series expansion in terms of the azimuthal angle. Various higher harmonics may be present due to e.g. the occurrence of multiple topological objects and their distributions over the entire transverse plane, the influence of transverse flow as well as the re-scattering of the CME current with medium. Here we concentrate the discussion on a possible measurement of the lowest harmonic that is most relevant to the CME current.

Let us next discuss how the above defined charge-dependent intrinsic single-particle distribution contributes to the charge-dependent azimuthal correlations recently measured by the STAR collaboration in [27]. Note that here we are only considering the contribution from the charge separation term in Eq. (10), while there are certainly additional contributions from two- and multi-particle correlations which we will discuss later in Section 4. Specifically the STAR collaboration has measured the following two- and three-particle correlations [27].

(i) The two-particle correlation $\langle \cos(\phi_i - \phi_j) \rangle$ for same-charge pairs ($++ / --$) and opposite-charge pairs ($+-$). The contribution to this correlator due to the charge-dependent intrinsic single-particle distribution, Eq. (10) is:

$$\delta_{++/--} \equiv \langle \cos(\phi_i - \phi_j) \rangle_{++/--} = d_1^2 \quad (11)$$

$$\delta_{+-} \equiv \langle \cos(\phi_i - \phi_j) \rangle_{+-} = -d_1^2 \quad (12)$$

(ii) The three-particle correlation $\langle \cos(\phi_i + \phi_j - 2\phi_k) \rangle$ for same-charge pairs ($i, j = ++ / --$) and opposite-charge pairs ($i, j = +-$) with the third particle, denoted by index k , having any charge. The contribution to these correlators due to the distribution, Eq. (10), turns out to be

$$\langle \cos(\phi_i + \phi_j - 2\phi_k) \rangle_{++/--, k-any} = v_2 d_1^2 \cos(2 \Delta\Psi_{CS}) \quad (13)$$

$$\langle \cos(\phi_i + \phi_j - 2\phi_k) \rangle_{+-, k-any} = -v_2 d_1^2 \cos(2 \Delta\Psi_{CS}) \quad (14)$$

where “k-any” indicates that the charge of the 3-rd particle may assume any value/sign. We have also defined the relative angle of the charged dipole with respect to the reaction plane, $\Delta\Psi_{CS} \equiv \Psi_{CS} - \Psi_{RP}$. The purpose of correlating the charged pair with the third particle is to address the reaction plane dependence of the pair-distribution, as discussed in the previous Section, Sect. 2.1. Indeed, the STAR collaboration has demonstrated [27] that the above three particle correlator is dominated by the reaction plane dependent two-particle correlation function $\langle \cos(\phi_i + \phi_j - 2\Psi_{RP}) \rangle$ and within errors they have found that

$$\langle \cos(\phi_i + \phi_j - 2\phi_k) \rangle = v_2 \langle \cos(\phi_i + \phi_j - 2\Psi_{RP}) \rangle \quad (15)$$

Based on the distribution Eq. (10) we find the same relation between these correlation functions, since the reaction-plane dependent two-particle correlation is given by

$$\gamma_{++/--} \equiv \langle \cos(\phi_i + \phi_j - 2\Psi_{RP}) \rangle_{++/--} = d_1^2 \cos(2\Delta\Psi_{CS}) \quad (16)$$

for same-charge pairs, and

$$\gamma_{+-} \equiv \langle \cos(\phi_i + \phi_j - 2\Psi_{RP}) \rangle_{+-} = -d_1^2 \cos(2\Delta\Psi_{CS}) \quad (17)$$

for opposite-charge pairs.

To make contact with the predictions of the CME for the above correlation functions, let us assume for the moment that an accurate identification of the reaction plane could be achieved. In this case we may rotate all events such that $\Psi_{RP} = 0$. Furthermore the CME predicts $\Delta\Psi_{CS} = \pi/2$, and thus, for $\Psi_{RP} = 0$ the charge separation term will take the form of $\sim d \sin(\phi)$ [16, 27, 28]. If the only contribution to the above correlations would be due to the CME, a very specific pattern arises:

$$\gamma_{++/--} = \langle \cos(\phi_i + \phi_j - 2\Psi_{RP}) \rangle_{++/--} = -d_1^2 < 0, \quad (18)$$

$$\delta_{++/--} = \langle \cos(\phi_i - \phi_j) \rangle_{++/--} = +d_1^2 > 0. \quad (19)$$

while

$$\gamma_{+-} = \langle \cos(\phi_i + \phi_j - 2\Psi_{RP}) \rangle_{+-} = +d_1^2 > 0, \quad (20)$$

$$\delta_{+-} = \langle \cos(\phi_i - \phi_j) \rangle_{+-} = -d_1^2 < 0. \quad (21)$$

This pattern for the correlations γ and δ , if seen in the data, would constitute a very strong evidence for occurrence of the CME in these collisions. However, as pointed out in [34], and as we shall discuss in more detail in Section 3 the STAR measurements do not show the above pattern. For example, while in the above analysis for the same-charge pairs the correlators γ and δ are expected to be equal in magnitude but *opposite* in sign, i.e., $\gamma_{++} = -\delta_{++}$ the

STAR data finds them approximately equal in magnitude but with the *same* (negative) sign.

2.3 The \hat{Q}_1^c vector analysis for measuring the charge separation

When exploring an important phenomenon such a local parity violation, it is very useful to develop multiple observables which test its predictions, such as the Chiral Magnetic Effect. This is particularly the case in the present situation. The signals due to the CME are expected to be rather weak and the observables are not free from various backgrounds due to “conventional” physics, such as two-particle correlations. In addition, the interpretation of the STAR data is rather ambiguous. Therefore, it will be very helpful to have an alternative observable which is sensitive to a possible charge separation with specific azimuthal orientation. Currently there are a few proposals, for example the \hat{Q}_1^c vector analysis [35], the charge multiplicity asymmetry correlations [36], and the out-of-plane charge asymmetry distribution [37]. Here we focus on a detailed discussion of the \hat{Q}_1^c vector analysis [35].

The \hat{Q}_1^c vector analysis aims at a direct measurement of the intrinsic charge-dependent distribution in Eq. (10) by identifying the charged dipole moment vector \hat{Q}_1^c of the final-state hadron distribution in the transverse momentum space. The magnitude Q_1^c and azimuthal angle Ψ_1^c of this vector can be determined in a given event by the following:

$$\begin{aligned} Q_1^c \cos \Psi_1^c &\equiv \sum_i q_i \cos \phi_i \\ Q_1^c \sin \Psi_1^c &\equiv \sum_i q_i \sin \phi_i \end{aligned} \quad (22)$$

where the summation is over all charged particles in the event, with q_i the electric charge and ϕ_i the azimuthal angle of each particle. This method is in close analogy to the \hat{Q}_1 and \hat{Q}_2 vector analysis used for directed and elliptic flow (see e.g. [30]). In the \hat{Q}_2 analysis one evaluates the charge independent quadrupole moment Q_2 and its direction Ψ_2 in a similar fashion

$$\begin{aligned} Q_2 \cos 2\Psi_2 &\equiv \sum_i \cos 2\phi_i \\ Q_2 \sin 2\Psi_2 &\equiv \sum_i \sin 2\phi_i \end{aligned} \quad (23)$$

The angle Ψ_2 is a measure for the reaction plane angle, Ψ_{RP} such that for a system with infinite many particles $\Psi_2 \rightarrow \Psi_{RP}$.

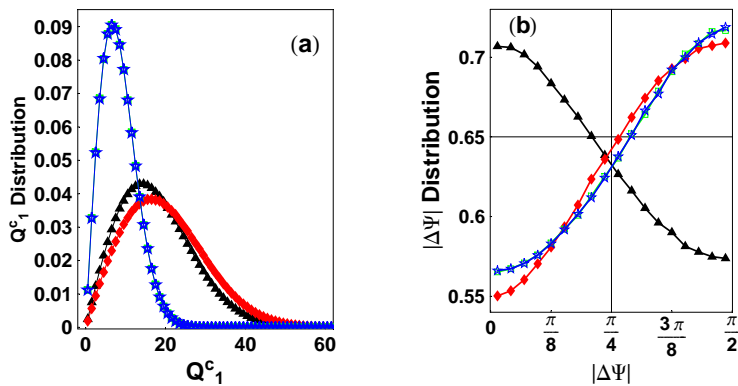


Fig. 2 (Color online) (a) The Q_1^c and (b) $|\Delta\Psi|$ distributions for the four different scenarios described in the text.

Contrary to \hat{Q}_2 , the charge dipole vector, \hat{Q}_1^c , incorporates the *electric charge* q_i of the particles. The mathematical details regarding the observable \hat{Q}_1^c and its relation to multi-particle correlations can be found in [35].

In each event, both angles Ψ_1^c and Ψ_2 are determined from a finite number of final state hadrons (see Fig. 1). While these angles correspond to their idealized expectations Ψ_{CS} and Ψ_{RP} only in the limit of infinite multiplicity, their distribution and in particular the distribution of their difference, $\Delta\Psi = \Psi_1^c - \Psi_2$ should provide a good estimator for the magnitude of the charged dipole angle with respect to the reaction plane, $\Delta\Psi_{CS} = \Psi_{CS} - \Psi_{RP}$.

The combined Q_1^c - and Q_2 - analysis will then provide distributions for the magnitude of the electric dipole, Q_1^c , and its relative angle with respect to Ψ_2 , $\Delta\Psi$. This is demonstrated in Fig. 2 where we show the distributions for various scenarios calculated in a Monte Carlo simulation [35].

- The black triangles correspond to a “benchmark” scenario, where we have only elliptic flow but neither a charged dipole nor any true pair correlations. Therefore the resulting distributions for Q_1^c and $|\Delta\Psi|$ arise only from pure statistical fluctuations.
- The red diamonds have been obtained by adding a physical dipole along the out-of-plane direction with a magnitude of $d_1 = 0.025$, to the benchmark scenario.
- The green boxes are based on the case where back-to-back angular correlation for about 1% of the same-charge pairs but no dipole have been added to the benchmark scenario.
- The blue stars result the case where same-side angular correlation for about 1% of the opposite-charge pairs but no dipole have been added to the benchmark scenario.

As can be seen from the comparison in Fig. 2 and a more detailed discussion in [35], only the combined analysis of the distributions of angle and

magnitude, is able to distinguish between scenarios based on conventional two-particle correlations and those involving a true charged momentum space dipole as predicted by the CME. As further discussed in [35] the final conclusion on the possible existence of an electric dipole will likely require a joint analysis of all three types of measurements, discussed in this Section: the Q_1^c distribution, the $\Delta\Psi$ distribution, as well as the charge-dependent azimuthal correlations γ and δ .

3 Interpretation of the available data

After having discussed the general aspects of charge dependent correlation functions in Section 2 we will now turn our attention to the actual measurements of such correlation function. Following the proposal by Voloshin [28] the STAR collaboration [27] presented the first measurement of the reaction-plane dependent charged-pair correlation function

$$\gamma_{\alpha,\beta} = \langle \cos(\phi_\alpha + \phi_\beta - 2\Psi_{RP}) \rangle \quad (24)$$

for pairs of particles with same, $(\alpha, \beta) = (+, +)$, $(-, -)$, and opposite charge, $(\alpha, \beta) = (+, -)$. As already discussed in the previous Section, in order to obtain the correlator $\gamma_{\alpha,\beta}$ STAR measured three-particle correlation functions, and demonstrated rather convincingly that, within errors, they are related to the reaction plane dependent two-particle charged-pair correlation function by

$$\langle \cos(\phi_\alpha + \phi_\beta - 2\phi_k) \rangle = v_2 \langle \cos(\phi_\alpha + \phi_\beta - 2\Psi_{RP}) \rangle = v_2 \gamma_{\alpha,\beta} \quad (25)$$

where v_2 denotes the measured elliptic flow parameter characterizing the elliptic azimuthal asymmetry. The results of the STAR measurement for $\gamma_{\alpha,\beta}$ are shown in the left panel of Fig. 3.

Since the relation, Eq. (25), has been established experimentally, we will concentrate our discussion on the charge dependent pair correlation function, $\gamma_{\alpha,\beta}$, Eq. (24). Furthermore, we will choose a frame where the reaction plane angle is set to zero, $\Psi_{RP} = 0$, so that

$$\gamma_{\alpha,\beta} = \langle \cos(\phi_\alpha + \phi_\beta) \rangle. \quad (26)$$

In this frame the in-plane direction coincides with the x-axis and the out-of-plane direction points along the y-axis. Also the average direction of the magnetic field will be along the y-axis.

Before we examine the STAR data more carefully let us recall what the prediction for the charge separation due to the Chiral Magnetic Effects are. As discussed in the previous section, the electric momentum space dipole induced by the CME will point (in an ideal situation) either parallel or anti-parallel to

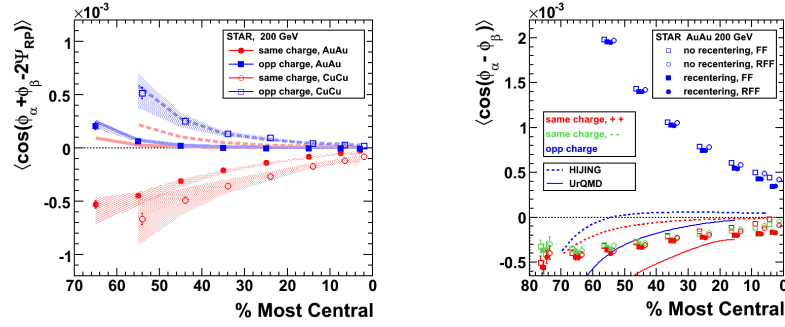


Fig. 3 The data from the STAR collaboration for the reaction plane dependent correlation function $\langle \cos(\phi_\alpha + \phi_\beta - 2\Psi_{RP}) \rangle$ (left) and the reaction-plane independent correlation function $\langle \cos(\phi_\alpha - \phi_\beta) \rangle$ (right) for like-sign and unlike-sign pairs. Also shown (lines) are results from various model calculations. The Figures are from [27].

the direction of the magnetic field, which in the frame where $\Psi_{RP} = 0$ points along the y -axis (neglecting fluctuations of the magnetic field [23]). Therefore, the charge separation due to the CME predicts to have pairs of same charge preferably moving together along the positive or negative y -direction. Pairs with opposite charge, on the other hand, are predicted to move away from each other along the y -axis. In terms of the azimuthal angles, ϕ_α, ϕ_β this means

$$(\phi_\alpha, \phi_\beta) = \left(\frac{\pi}{2}, \frac{\pi}{2}\right) \text{ or } \left(\frac{3\pi}{2}, \frac{3\pi}{2}\right) \quad (27)$$

for same-charge pairs, and

$$(\phi_\alpha, \phi_\beta) = \left(\frac{\pi}{2}, \frac{3\pi}{2}\right) \text{ or } \left(\frac{3\pi}{2}, \frac{\pi}{2}\right) \quad (28)$$

for opposite-charge pairs. Since

$$\cos\left(\frac{\pi}{2} + \frac{\pi}{2}\right) = \cos\left(\frac{3\pi}{2} + \frac{3\pi}{2}\right) = -1 \quad (29)$$

$$\cos\left(\frac{3\pi}{2} + \frac{\pi}{2}\right) = 1 \quad (30)$$

the correlation function $\gamma_{\alpha,\beta}$, Eq. (26), is expected to be negative for same-charge pairs and positive for opposite-charge pairs. While the STAR data, shown in Fig. 3, indeed show a negative value for same-charge pairs, the result for opposite-charge pairs is, at best, only mildly positive and, within errors, compatible with zero. Since opposite charged pairs are predicted to move away from each other, one may argue their (anti-) correlation should be weakened as these particles will have to traverse the entire fireball [13].

Therefore, at first sight, the STAR data may indeed show a first evidence for the charge separation pattern as predicted by the CME. However, the interpretation of the data is more difficult.

The complication arises from the fact that the correlation function $\gamma_{\alpha,\beta}$ does not unambiguously determine the angular correlation of the pair. To see this, consider a same-charge pair with angles $(\phi_\alpha, \phi_\beta) = (0, \pi)$. In this case the particles move away from each other in the in-plane direction. This is just the opposite of the correlation predicted by the CME, where the two particles are moving with each other in the out-of-plane direction. For both cases we get

$$\cos(\phi_\alpha, \phi_\beta) = \cos(0 + \pi) = \cos\left(\frac{\pi}{2} + \frac{\pi}{2}\right) = -1. \quad (31)$$

Thus, the correlation function $\gamma_{\alpha,\beta}$ is *not* able to distinguish between same-side out-of-plane correlations and back-to-back in-plane correlations. However, this ambiguity can easily be resolved by considering the reaction plane independent correlation function

$$\delta_{\alpha,\beta} = \langle \cos(\phi_\alpha - \phi_\beta) \rangle \quad (32)$$

which STAR has also measured, and we show their results in the right panel of Fig. 3. In the frame, where $\Psi_{RP} = 0$, the two correlation functions may be decomposed in the in-plane $\sim \langle \cos(\phi_\alpha) \cos(\phi_\beta) \rangle$ and out-of-plane $\sim \langle \sin(\phi_\alpha) \sin(\phi_\beta) \rangle$ components:

$$\begin{aligned} \gamma_{\alpha,\beta} &= \langle \cos(\phi_\alpha + \phi_\beta) \rangle = \langle \cos(\phi_\alpha) \cos(\phi_\beta) \rangle - \langle \sin(\phi_\alpha) \sin(\phi_\beta) \rangle, \\ \delta_{\alpha,\beta} &= \langle \cos(\phi_\alpha - \phi_\beta) \rangle = \langle \cos(\phi_\alpha) \cos(\phi_\beta) \rangle + \langle \sin(\phi_\alpha) \sin(\phi_\beta) \rangle. \end{aligned} \quad (33)$$

Qualitatively the STAR measurement in Au+Au collisions for both these correlation functions, $\gamma_{\alpha,\beta}$ and $\delta_{\alpha,\beta}$ for same-sign and opposite-sign pairs of charged particles, may be characterized as follows (see Fig. 3):

- For same-sign pairs:

$$\langle \cos(\phi_\alpha + \phi_\beta) \rangle_{same} \simeq \langle \cos(\phi_\alpha - \phi_\beta) \rangle_{same} < 0. \quad (34)$$

Using Eq. (33) this implies

$$\begin{aligned} \langle \sin(\phi_\alpha) \sin(\phi_\beta) \rangle_{same} &\simeq 0, \\ \langle \cos(\phi_\alpha) \cos(\phi_\beta) \rangle_{same} &< 0. \end{aligned} \quad (35)$$

- For opposite-sign pairs we find that

$$\begin{aligned} \langle \cos(\phi_\alpha + \phi_\beta) \rangle_{opposite} &\simeq 0 \\ \langle \cos(\phi_\alpha - \phi_\beta) \rangle_{opposite} &> 0. \end{aligned} \quad (36)$$

Again, using Eq. (33), this means

$$\langle \sin(\phi_\alpha) \sin(\phi_\beta) \rangle_{opposite} \simeq \langle \cos(\phi_\alpha) \cos(\phi_\beta) \rangle_{opposite} > 0. \quad (37)$$

The decomposition of the actual data into the in-plane and out-of-plane components is shown in Fig. 4. Obviously the correlations for same-charge

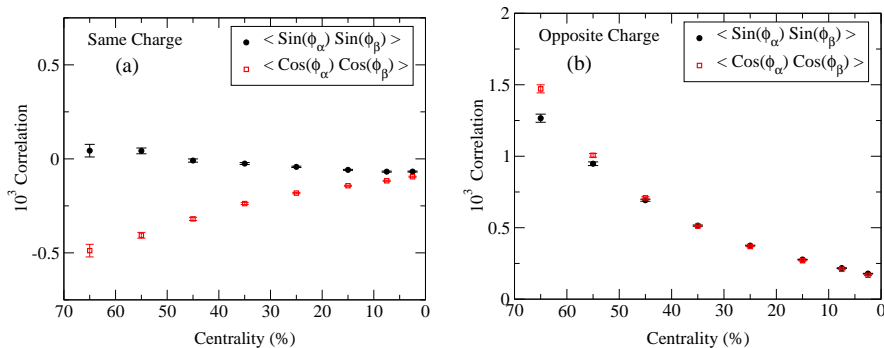


Fig. 4 Correlations in-plane $\langle \cos(\phi_\alpha) \cos(\phi_\beta) \rangle$ and out-of-plane $\langle \sin(\phi_\alpha) \sin(\phi_\beta) \rangle$ for same- and opposite-charge pairs in $Au + Au$ collisions as seen in the STAR data.

pairs are predominantly in-plane and back-to-back. This is exactly the *opposite* of what has been predicted by the Chiral Magnetic Effect. This is illustrated in Fig. 5 where we have sketched the experimental situation for same-charge pairs based on the STAR data. For pairs with opposite charge, both in-plane and out-of-plane correlations have the same (positive) sign and magnitude. This implies that opposite-charged pairs move together equally likely in the in-plane and out-of-plane directions. This behavior can at least qualitatively be understood by resonance/cluster decays [36] or local charge conservation [38].

In addition to the data shown in Fig. 3, STAR has also analyzed the reaction plane dependent correlation function $\gamma_{\alpha,\beta}$ differentially as a function of the pair transverse momentum (sum and difference) and rapidity difference. Both these results are within qualitative expectations for a charge separation effect due to the CME [34]. Unfortunately, similar differential information is not available for the reaction plane independent correlation function, $\delta_{\alpha,\beta}$. Therefore a differential decomposition into in-plane and out-of-plane components, as we have done here, unfortunately is not possible at this time. Such information may help to further constrain possible background effects as well as predictions from the CME.

Recently, the ALICE collaboration reported [39] the measurement of the same correlation functions for Pb+Pb collisions at a center of mass energy of $\sqrt{s} = 2.76$ TeV, about ten times that of the STAR measurement. Just like STAR, ALICE determined the reaction plane dependent correlation function

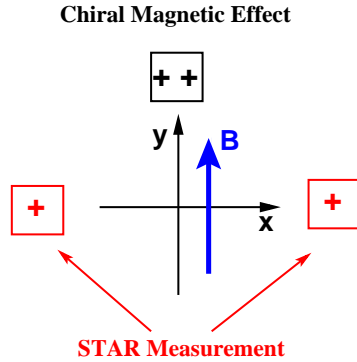


Fig. 5 Schematic illustration of the actual STAR measurement (red) together with the predictions from the Chiral Magnetic Effect (black) for same-charge pairs.

$\gamma_{\alpha,\beta}$ integrated over transverse momentum and rapidity as well as differentially. Within errors, the data for the integrated correlation function $\gamma_{\alpha,\beta}$ agree with those of the STAR measurement, and the differential measurement show the same qualitative features.

For the reaction plane independent correlation function, $\delta_{\alpha,\beta}$, on the other hand, the ALICE data differ from those by STAR. In particular, ALICE finds this correlation function to be positive for *both* opposite- and same-charge pairs. ALICE also provides the in-plane and out-of-plane pair correlations, $\langle \cos(\phi_\alpha) \cos(\phi_\beta) \rangle$ and $\langle \sin(\phi_\alpha) \sin(\phi_\beta) \rangle$, respectively. Similar to the STAR measurement ALICE finds that for opposite-charge pairs the in- and out-of-plane correlations are nearly identical and positive. For the same-charge pairs, however, ALICE finds both in- and out-of-plane projections to be positive, with the out-of-plane correlation slightly larger than the in-plane projection. This finding would be in qualitative agreement with the expectations from the CME. Amusingly, early predictions [40] for the collision energy dependence of the CME expected a smaller effect at the very high energies where ALICE has been measuring, largely due to the shorter duration of the magnetic field. Of course the complex dynamics of heavy ion collisions and the various background contributions turn quantitative predictions for these correlation functions into a very difficult task, and a final resolution will require a systematic analysis of all available data at various energies.

Given that the STAR data show an in-plane back-to-back correlation for same-sign pairs, one may wonder if there is still room for a charge separation effect due to the CME. This has been analyzed in [34] with the result that for the transverse momentum and rapidity integrated data, which the above analysis is based on, the backgrounds need to exactly cancel the CME induced charge separation. This may be just a coincidence, however. After all the data by ALICE show a different trend for the same-sign correlations. For

this situation to be clarified further differential data for the reaction plane independent correlation function, $\delta_{\alpha,\beta}$ are required for both collision energies.

Finally, as part of the RHIC beam energy scan program, STAR has measured the reaction-plane dependent correlator $\gamma_{\alpha,\beta}$ for various collision energies [41], see also [26]. They find that the difference for the correlator between same-sign and opposite-sign pairs decreases with decreasing beam energy. Such a behavior is expected from the CME. However, as we will discuss in the next section, all background terms scale with the elliptic flow parameter, v_2 , which is known to decrease with decreasing collision energy as well.

To conclude this section, presently available experimental results concerning the CME are inconclusive. While the integrated STAR data disfavor the presence of the CME, the ALICE data allow for more positive conclusions. Clearly, progress requires data at lower energies as well as, and most importantly, differential measurements of both the reaction plane dependent and reaction plane independent correlation functions. In addition, given the rather unsettled state of affairs, measurements of other observables, such as the one proposed in the previous section, would be very welcome.

4 Discussion of various background contributions

As discussed in the previous sections the Chiral Magnetic Effect (CME) - if it exists - contributes to the reaction plane dependent two-particle correlator, first introduced in [28]. As in the previous section we denote the reaction plane dependent two-particle correlator by

$$\gamma \equiv \langle \cos(\phi_1 + \phi_2 - 2\Psi_{RP}) \rangle, \quad (38)$$

where ϕ_1 and ϕ_2 are the azimuthal angles of two particles, and Ψ_{RP} is the reaction plane angle. In the following we will distinguish between $\gamma_{++/--}$, γ_{+-} and γ denoting respectively the correlator (38) for same-sign pairs, opposite-sign pairs, and the correlator without specifying the sign of measured particles.

As discussed in Section 3 a detailed measurement of γ was performed both at RHIC by the STAR collaboration [27] and at the LHC by the ALICE collaboration [39]. However, as already discussed in the previous Section, the interpretation of experimental data is not straightforward since various effects can contribute to γ .

The presence of elliptic flow allows for practically all “conventional” two-particle correlations to contribute to the reaction-plane dependent correlation function, γ . This can be easily seen from the decomposition of γ into in-plane and out-of-plane projections, Eq. (33)

$$\gamma = \langle \cos(\phi_1) \cos(\phi_2) \rangle - \langle \sin(\phi_1) \sin(\phi_2) \rangle. \quad (39)$$

It is quite obvious that even if the underlying correlation mechanism does not depend on the reaction plane it will contribute to γ in the presence of the elliptic anisotropy v_2 . This can be seen in an extreme, though unrealistic, situation where all particles are produced exactly in-plane. In this case $\langle \sin(\phi_1) \sin(\phi_2) \rangle = 0$ simply because there are no particles in the out-of-plane direction and $\gamma = \langle \cos(\phi_1) \cos(\phi_2) \rangle$. Obviously in this case, the presence of any two-particle angular correlation mechanism will result in a non-zero value of γ .

In this Section we will focus exclusively on the contribution to γ driven by the non-vanishing elliptic anisotropy v_2 . First we will derive the general expression which relates the elliptic anisotropy and the correlator γ in the presence of arbitrary two-particle correlations. Next we will discuss a few explicit mechanisms that need to be understood quantitatively, before any conclusions about the existence of the CME can be made. In particular we will address corrections due to transverse momentum conservation (TMC) [42, 43, 44] and the local charge conservation [38], both of which appear to contribute significantly to γ . In the last part of the paper we will discuss the possibility of removing, in the model independent way, the elliptic-flow-related background from γ .

4.1 General relation

In this part we derive the general relation between the elliptic anisotropy v_2 and the two-particle correlator γ in the presence of an arbitrary reaction plane independent two-particle correlations.

By definition, the two-particle correlator γ is

$$\gamma = \frac{\int \rho_2(\phi_1, \phi_2, x_1, x_2, \Psi_{RP}) \cos(\phi_1 + \phi_2 - 2\Psi_{RP}) d\phi_1 d\phi_2 dx_1 dx_2}{\int \rho_2(\phi_1, \phi_2, x_1, x_2, \Psi_{RP}) d\phi_1 d\phi_2 dx_1 dx_2}, \quad (40)$$

where, to simplify our notation, we denote: $x = (p_t, \eta)$ and $dx = p_t dp_t d\eta$. Here p_t is the absolute value of transverse-momentum, while η is pseudorapidity (or rapidity). ρ_2 is the two-particle distribution in the intrinsic frame with the reaction plane angle Ψ_{RP} . It can be expressed in terms of the single-particle distributions, and the underlying correlation function C (see Section 2)

$$\rho_2(\phi_1, \phi_2, x_1, x_2, \Psi_{RP}) = \rho(\phi_1, x_1, \Psi_{RP}) \rho(\phi_2, x_2, \Psi_{RP}) [1 + C(\phi_1, \phi_2, x_1, x_2)]. \quad (41)$$

To simplify our calculation we assume the single-particle distribution to be

$$\rho(\phi, x, \Psi_{RP}) = \frac{\rho_0(x)}{2\pi} [1 + 2v_2(x) \cos(2\phi - 2\Psi_{RP})], \quad (42)$$

where $\rho_0(x)$ and $v_2(x)$ depend solely on $x = (p_t, \eta)$. We neglect higher moments v_n since their contribution to γ turns out to be proportional to $v_n v_m$ which is much smaller than the leading term $\sim v_2$, see Ref. [45].

If $v_2(x) \neq 0$, the single particle distributions depend on the reaction plane. Therefore, the part of the two-particle density (41) involving the two-particle correlation function C depends on the reaction plane even if C depends only on $\phi_1 - \phi_2$.

Here we want to concentrate on those correlations that depend only on $\Delta\phi = \phi_1 - \phi_2$, namely the underlying correlation mechanism is insensitive to the reaction plane orientation. The correlation function may be expanded in a Fourier series

$$C(\Delta\phi, x_1, x_2) = \sum_{n=0}^{\infty} a_n(x_1, x_2) \cos(n\Delta\phi), \quad (43)$$

where $a_n(x_1, x_2)$ does not depend on ϕ_1 and ϕ_2 . Substituting (43) and (41) into Eq. (40), we obtain

$$\gamma = \frac{1}{2N^2} \int \rho_0(x_1)\rho_0(x_2)a_1(x_1, x_2)[v_2(x_1) + v_2(x_2)]dx_1dx_2, \quad (44)$$

where $N = \int \rho_0(x)dx$, and we have assumed that $a_n \ll 1$.

Equation (44) explains why all correlation mechanisms with a non-zero $a_1(x_1, x_2)$ contribute to γ . For instance, it has been shown that transverse momentum conservation (TMC) leads to a correlation function which depends on $\cos(\Delta\phi)/N_{\text{tot}}$ [46], where N_{tot} is the total number of produced particles. In this case $a_1(x_1, x_2) \propto 1/N_{\text{tot}}$. Let us also emphasize that all correlations that depend on the momentum difference between particles $\Delta k = |\mathbf{k}_1 - \mathbf{k}_2|$ also contribute to γ . In this case:

$$C(\Delta k) = C(k_1^2 + k_2^2 - 2k_1k_2 \cos(\Delta\phi)), \quad (45)$$

which naturally leads to a non-vanishing a_1 term.

To summarize, Eq. (44) explains why transverse-momentum conservation [42, 43, 44], local charge-conservation [38], resonance- (cluster-) decay [36], and all other correlations with $\Delta\phi$ dependence contribute to γ .

4.2 Transverse momentum conservation

Very soon after publication of the experimental data by the STAR Collaboration it was realized that transverse momentum conservation convoluted with the non-zero elliptic anisotropy can lead to a substantial corrections for γ [47, 43, 42]. This can be easily seen for the simplified situation where all particles are measured (in the full phase-space), and where they all have exactly the same magnitude of transverse momentum $|\mathbf{p}_{i,t}| = |\mathbf{p}_t|$, $i = 1, \dots, N_{\text{tot}}$.

In the frame where $\Psi_{RP} = 0$ the correlator γ may be written as

$$\gamma = \left\langle \frac{\sum_{i \neq j} \cos(\phi_i + \phi_j)}{\sum_{i \neq j} 1} \right\rangle, \quad (46)$$

or, alternatively,

$$\gamma = \left\langle \frac{(\sum_i \cos(\phi_i))^2 - (\sum_i \sin(\phi_i))^2 - \sum_i \cos(2\phi_i)}{\sum_{i \neq j} 1} \right\rangle, \quad (47)$$

where i and j are summed over all particles in the full phase-space. In the simplified scenario, where $|\mathbf{p}_{i,t}| = |\mathbf{p}_t|$, the conservation of transverse momentum implies

$$\sum_i \cos(\phi_i) = \sum_i \sin(\phi_i) = 0. \quad (48)$$

Consequently we obtain

$$\gamma = - \left\langle \frac{\sum_i \cos(2\phi_i)}{N_{\text{tot}}(N_{\text{tot}} - 1)} \right\rangle \approx \frac{-v_2}{N_{\text{tot}}}, \quad (49)$$

where N_{tot} is the total number of particles. Taking, for example, the centrality class 40 – 50% we approximately have $v_2 \approx 0.1$ and $N_{\text{tot}} \approx 1500$ leading to $\gamma \approx -0.7 \cdot 10^{-4}$ from TMC. This is roughly a factor 3 – 4 smaller than the experimental data for the same-charge pairs. This is only a simple estimation and a more realistic AMPT calculations [44] suggest that the TMC contribution is roughly factor 2 smaller than the STAR data.

In a similar way we obtain for the reaction plane independent correlation function

$$\delta = \langle \cos(\phi_1 - \phi_2) \rangle \approx -\frac{1}{N_{\text{tot}}}. \quad (50)$$

In this case for $N_{\text{tot}} \approx 1500$ we obtain $\delta \approx -0.7 \cdot 10^{-3}$ which is comparable or slightly larger in magnitude than same-charge data by the STAR collaboration.

Similar results hold also in a more realistic situation, where only a small fraction of all particles is measured, and the magnitudes of transverse momenta are distributed according to the thermal distribution. This has been discussed in detail in [43], and we will only show the most important results.

Using the central limit theorem and implying the global conservation of transverse momentum, the two-particle distribution function reads [46, 48, 43]

$$\rho_2(\mathbf{p}_1, \mathbf{p}_2) \simeq \rho(\mathbf{p}_1)\rho(\mathbf{p}_2) \left(1 + \frac{2}{N_{\text{tot}}} - \frac{(p_{1,x} + p_{2,x})^2}{2N_{\text{tot}} \langle p_x^2 \rangle_F} - \frac{(p_{1,y} + p_{2,y})^2}{2N_{\text{tot}} \langle p_y^2 \rangle_F} \right). \quad (51)$$

where x and y denote the two components of transverse momentum. F denotes that the appropriate average is calculated for all particles in the full phase-space. The single particle distribution, $\rho(\mathbf{p}_1)$, is given by Eq. (42).

Before we continue let us clarify one subtle point. Equation (51) is derived assuming that we first sample particles with a given v_2 and next we conserve transverse momentum for all particles. In reality the opposite scenario should be considered. First we should sample partons/particles with a conserved transverse momentum, and after this the elliptic anisotropy v_2 should be generated according to some dynamical model. Of course the second approach is much more challenging and renders analytical calculations difficult. At the end of this Section we will show that both procedures lead to comparable results for γ and δ and their transverse momentum distributions, however the rapidity distributions are quite different. We will come back to this point later.

Using Eq. (51) and Eq. (40) we can derive the following relations for γ and δ :

$$\gamma = -\frac{1}{N_{\text{tot}}} \frac{\langle p_t \rangle_{\Omega}^2}{\langle p_t^2 \rangle_F} \frac{2\bar{v}_{2,\Omega} - \bar{v}_{2,F} - \bar{v}_{2,F}(\bar{v}_{2,\Omega})^2}{1 - (\bar{v}_{2,F})^2}, \quad (52)$$

and

$$\delta = -\frac{1}{N_{\text{tot}}} \frac{\langle p_t \rangle_{\Omega}^2}{\langle p_t^2 \rangle_F} \frac{1 + (\bar{v}_{2,\Omega})^2 - 2\bar{v}_{2,F} \bar{v}_{2,\Omega}}{1 - (\bar{v}_{2,F})^2}, \quad (53)$$

where we have introduced certain weighted moments of v_2 :

$$\bar{v}_2 = \frac{\langle v_2(p_t, \eta) p_t \rangle}{\langle p_t \rangle}, \quad \bar{\bar{v}}_2 = \frac{\langle v_2(p_t, \eta) p_t^2 \rangle}{\langle p_t^2 \rangle}. \quad (54)$$

In the above equations F and Ω denote averages that are calculated for all particles in the full phase-space, or for all actually measured particles in the restricted phase-space, respectively. Performing explicit calculations with reasonable assumptions about p_t and η dependence of the single-particle distribution $\rho(p_t, \eta)$ and elliptic flow $v_2(p_t, \eta)$, we have found that for mid-central and peripheral collisions [43]

$$\gamma \cdot N_{\text{part}} \approx -0.005, \quad \delta \cdot N_{\text{part}} \approx -0.05, \quad (55)$$

where N_{part} is the number of participants, also referred to as wounded nucleons [49].

To summarize, transverse momentum conservation results in a negative contributions to both γ and δ , and they are of the same order of magnitude as the experimental measurement for like-sign pairs. More precisely they are a factor of 3 – 5 (very peripheral – mid-central) less in magnitude for γ , and a factor 1.5 – 4 (mid-central – very peripheral) larger for δ than the STAR data for the same-sign correlator. While it is rather difficult to understand the data with only transverse momentum conservation it is interesting to

notice that the STAR experiment is sensitive enough to the effect of global transverse momentum conservation.

Using Eqs. (40,51) we can easily calculate the dependence of γ and δ on the sum $p_+ = (p_{1,t} + p_{2,t})/2$ and difference $p_- = |p_{1,t} - p_{2,t}|/2$ of the transverse momenta of the pair. For the STAR data [27], γ is growing roughly linearly with p_+ and is approximately constant as a function of p_- . Interestingly a

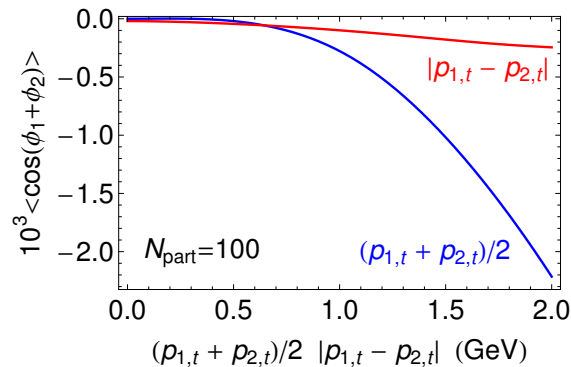


Fig. 6 The two-particle azimuthal correlator $\langle \cos(\phi_1 + \phi_2) \rangle$ vs $p_+ = (p_{1,t} + p_{2,t})/2$ (blue line) and $p_- = |p_{1,t} - p_{2,t}|$ (red line) for $N_{part} = 100$. The results are in qualitative and partly quantitative agreement with the STAR data for the same-charge correlator. Figure from Ref. [43].

very similar behavior is obtained in the scenario with only global transverse momentum conservation. As seen in Fig. 6, the contribution of TMC to γ is consistent with the data for $p_+ > 1$ GeV and underestimates the data for $p_+ < 1$ GeV. As expected, for δ very similar dependence on p_+ and p_- is obtained but rescaled by a value of v_2 .

Recently, very similar results were obtained in the AMPT model calculation [44], where the transverse momentum is conserved on the event-by-event basis, and we will come back to this point later.

4.2.1 Pseudorapidity dependence

Since the contribution to γ due to transverse momentum conservation is proportional to v_2 , one would naively expect that its (pseudo)rapidity dependence trace the rather mild (pseudo)rapidity dependence of v_2 .

However, as shown in Ref. [42], under quite reasonable assumptions we can obtain very similar rapidity dependence as in the experimental data. In the STAR measurement [27] the correlator γ is maximum for $|\eta_1 - \eta_2| = 0$ and is approximately linearly decreasing to values consistent with zero at $|\eta_1 - \eta_2| \approx 2$.

For simplicity of the argument let us assume that at the time $t = 0$ all produced partons/particles are distributed between two separate bins in rapidity with enforced global transverse momentum conservation. It means that if in the first bin the total transverse momentum equals $\mathbf{K}_{1,t}$, in the second bin $\mathbf{K}_{2,t} = -\mathbf{K}_{1,t}$ in each event. Assuming further that all particles have the same magnitude of transverse momentum $|\mathbf{p}_{i,t}| = |\mathbf{p}_t|$, $i = 1, \dots, N_{\text{tot}}$, we obtain the following relation

$$\gamma \propto \left\langle \sum_{i \in 1} \cos(\phi_i) \sum_{k \in 2} \cos(\phi_k) - \sum_{i \in 1} \sin(\phi_i) \sum_{k \in 2} \sin(\phi_k) \right\rangle, \quad (56)$$

and

$$\gamma \propto \langle K_{x,1}K_{x,2} - K_{y,1}K_{y,2} \rangle = \langle K_{y,1}^2 - K_{x,1}^2 \rangle, \quad (57)$$

where x and y denote the components of transverse momentum. It should be noted that here we calculate the two-particle correlator where one particle is taken from a bin number 1, and the second particle from a bin number 2.

Now let us evaluate γ at time $t=0$. In this case it is reasonable to assume that there is no elliptic anisotropy v_2 and $\gamma = 0$ by definition. If we assume that bins are separated enough in rapidity so that there is no momentum exchange between two bins during the fireball evolution, i.e., the total transverse momentum $\mathbf{K}_{1,t}$ is constant, then $\gamma = 0$ also in the final state, even if subsequently a non-zero v_2 is generated. Of course this simple argument demonstrates only that having the global TMC we can still obtain a non-trivial dependence of γ as a function of $\eta_1 - \eta_2$. In Ref. [42] this problem was studied in detail in the cascade model, where it was shown that the satisfactory description of the data can be obtained.

We conclude that although the TMC probably cannot explain the data completely it gives rise to contributions which are of the same order of magnitude and which exhibit both the transverse momentum and rapidity dependence in qualitative and partly quantitative agreement with the STAR data.

4.3 AMPT model

It is desirable to study the correlators γ and δ also in an advanced Monte Carlo model, which allows for the conservation of transverse momentum on the event-by-event basis, and which generates reasonable values for the elliptic anisotropy v_2 . Recently such calculation was performed in the AMPT model and the results are presented in Ref. [44] with the conclusion that the signal coming from AMPT is dominated by TMC. Indeed, the obtained results, summarized in Figs. 7 and 8, are in very good agreement with the previous discussion. As seen in Fig. 7, the calculated correlator γ is in a good

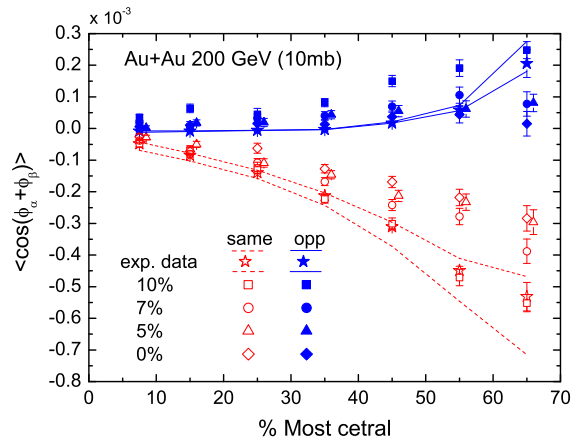


Fig. 7 The two-particle azimuthal correlator γ as a function of centrality in the AMPT model with different values of initial charge separation.

qualitative agreement with the data, however it underestimates the STAR data by a factor of ~ 2 . It was also shown that initializing the AMPT calculation with the charge dipole leads to a better description of the data.

In Fig. 8 the correlator γ is plotted as a function of $p_+ = (p_{1,t} + p_{2,t})/2$ and $\Delta\eta = \eta_1 - \eta_2$. Again, qualitatively the AMPT model reproduce the data but underestimate it by a factor of 2.

As seen from the figures the AMPT model calculation (without initial dipole) is consistent with the global TMC and allows to understand the behavior of the STAR data. It clearly demonstrates that all possible background effects must be studied very thoroughly before any conclusion about local parity violation can be reached.

4.4 Local charge conservation

Given the previous discussion, it is useful to construct a two-particle correlator which is insensitive to transverse momentum conservation and other charge independent correlations. The natural choice is the difference of opposite-sign and same-sign pair correlator (38), see [38]:

$$\gamma_P \equiv \frac{1}{2}(2\gamma_{+-} - \gamma_{++} - \gamma_{--}). \quad (58)$$

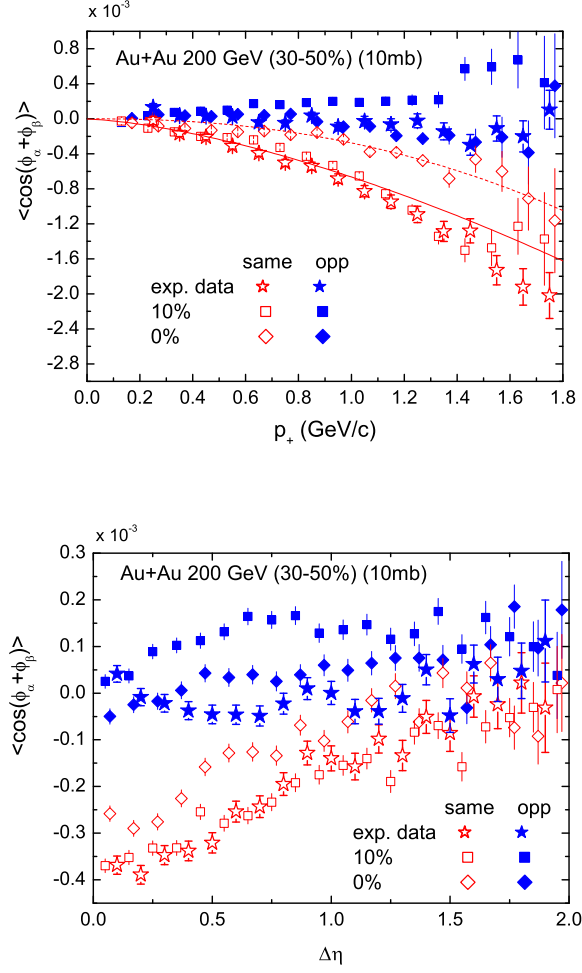


Fig. 8 The two-particle azimuthal correlator γ as a function of $p_+ = (p_{1,t} + p_{2,t})/2$ and $\Delta\eta = \eta_1 - \eta_2$ in the AMPT model with different initial values of charge separation.

It is clear that only correlations that are charge sensitive will contribute to γ_P . While the CME, if present, will contribute to γ_P , global TMC, for example will not. Therefore the successful description of γ_P with conventional physics would constitute a serious challenge for the interpretation of the data in terms of the CME.

In Ref. [38] it was argued that γ_P can be fully understood assuming that charges are produced later in the collision (delayed hadronization). Indeed,

in the calculation of Ref. [38] the charges are produced in pairs in the same point in space-time. Due to the collective flow the initial correlation in space-time is translated into correlations in momentum space, and consequently it contributes to γ_P . In this approach particles are emitted according to the blast-wave model with the additional requirement of local charge conservation at freeze-out. Local charge balance is enforced within the finite range in rapidity σ_η and the azimuthal angle σ_ϕ . By comparing the model with experimental data on the balance function [50], the values of σ_η and σ_ϕ can be extracted which allows to make prediction for γ_P .

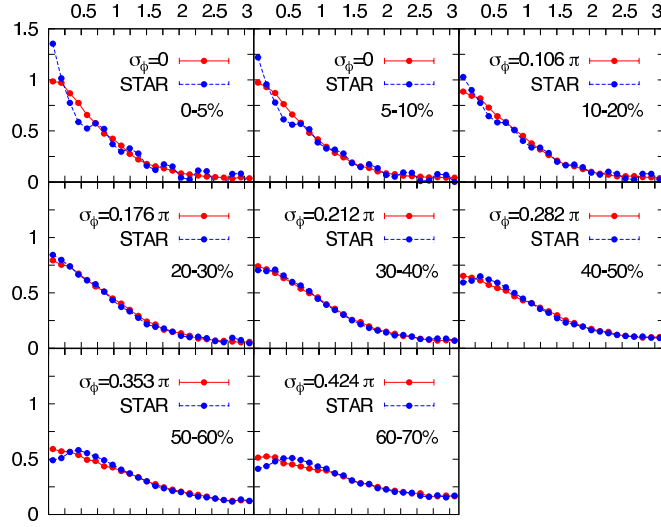


Fig. 9 Model with a delayed charge production and the local charge conservation vs the STAR data on the balance function in the relative azimuthal angle $\Delta\phi = \phi_1 - \phi_2$.

The details of this calculation are presented in Ref. [38]. Here we summarize only the main results. It turns out that the model with delayed charge creation and local charge conservation can provide a successful description of the balance function both in the relative angle $\Delta\phi = \phi_1 - \phi_2$ and the relative pseudorapidity $\Delta\eta$, see Fig. 9 as an example.³

Using the best values of parameters σ_η and σ_ϕ the contribution of local charge conservation to γ_P can be calculated. The results are presented in Fig. 10.

As seen in Fig. 10 the agreement of the model with the STAR data is very good. It suggests that the two-particle charge sensitive correlations may be dominated by the local charge conservation.

³ Recently a similar model was proposed to explain the fall-off of the same-side ridge in $\Delta\eta$ [51].

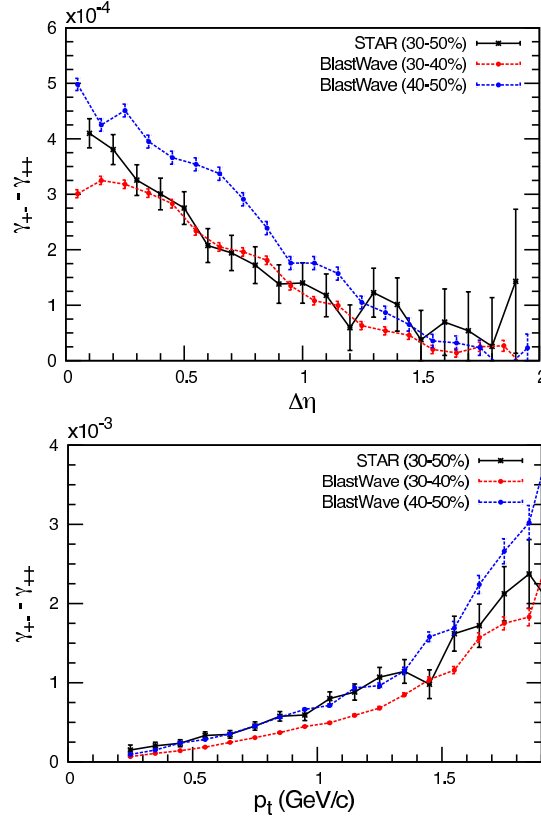


Fig. 10 Model with a delayed charge production and local charge conservation vs the STAR data on γ_P as a function of p_+ and $\Delta\eta$.

4.5 Decomposition of flow-induced and flow-independent contributions

From the analysis of the data in Section 3 as well as the discussion of various “background” effects, it appears rather plausible that the observed charge-dependent correlation patterns in γ and δ contain contributions from more than one source. In particular there are effects whose contributions to these correlations are flow-dependent, for example the transverse momentum conservation (TMC) or the local charge conservation (LCC). On the other hand the CME, if present, is flow independent. Let us, therefore, attempt a decomposition of flow-induced and flow-independent contributions.

We first consider correlation effects where the underlying correlation function C is independent of the reaction plane orientation:

$$\mathcal{C}(\phi_1, \phi_2) \propto \rho(\phi_1, \Psi_{RP})\rho(\phi_2, \Psi_{RP})\mathcal{C}(\phi_1 - \phi_2), \quad (59)$$

where ρ is a single particle distribution. Note that the above is true for both TMC and LCC effects. A correlation effect of this type will contribute to the measured correlators as follows:

$$\gamma_{\alpha,\beta} \sim v_2 F_{\alpha,\beta} \quad , \quad \delta_{\alpha,\beta} \sim F_{\alpha,\beta}, \quad (60)$$

with the factor $F_{\alpha,\beta}$ representing the strength of the effects, and (α, β) is either $++ / --$ or $+-$. Both the TMC and the LCC follow this pattern albeit with opposite contributions. Thus F represents the total of all effects of this type.

We should note, however, that the above relation, Eq. (60) is a simplification of the exact relation between γ and $v_2(p_t, \eta)$, which is given in Eq. (44). Since the purpose of the present discussion is to gain some qualitative insight into the various contributions, we assume here that γ is approximately proportional to the integrated v_2 .

Next we consider possible contributions of the CME type. They would appear in the two-particle density in the following form

$$\rho_2(\phi_1, \phi_2) \propto \sin(\phi_1 - \Psi_{RP}) \sin(\phi_2 - \Psi_{RP}), \quad (61)$$

which explicitly involves the reaction plane. This term will contribute to the measured correlators as follows:

$$\gamma_{\alpha,\beta} \sim -H_{\alpha,\beta} \quad , \quad \delta_{\alpha,\beta} \sim H_{\alpha,\beta}, \quad (62)$$

with the factor H representing the strength of the effects. It should be pointed out that besides the CME, there are possibly other effects that may also contribute to the correlators with the above pattern. One example is a possible dipole asymmetry from initial condition fluctuations that preferably aligns with the out-of-plane direction, see Ref. [52] for details. However, this effect will be charge independent, i.e., $H_{++/--} = H_{+-} > 0$, whereas the CME predicts a charge dependence, $H_{++/--} = -H_{+-} > 0$.

Combining the two types of contributions we arrive at the following decomposition for the reaction plane dependent and independent correlation functions,

$$\gamma_{\alpha,\beta} \sim v_2 F_{\alpha,\beta} - H_{\alpha,\beta} \quad , \quad \delta_{\alpha,\beta} \sim F_{\alpha,\beta} + H_{\alpha,\beta}. \quad (63)$$

Given these relations, we may use the STAR data for $\gamma_{\alpha,\beta}$, $\delta_{\alpha,\beta}$, and v_2 to extract the strength factors $F_{\alpha,\beta}$ and $H_{\alpha,\beta}$ as a function of centrality. The result of such a decomposition is shown in Fig. 11.

Given this analysis we make the following observations: (a) Both components are charge dependent, i.e. there is significant difference between $++/--$ and $+-$; (b) In both cases, however, the same-charge and opposite-charge signals are not symmetric with respect to zero. This may indicate that in each category there are likely more than one source of correlations; (c)

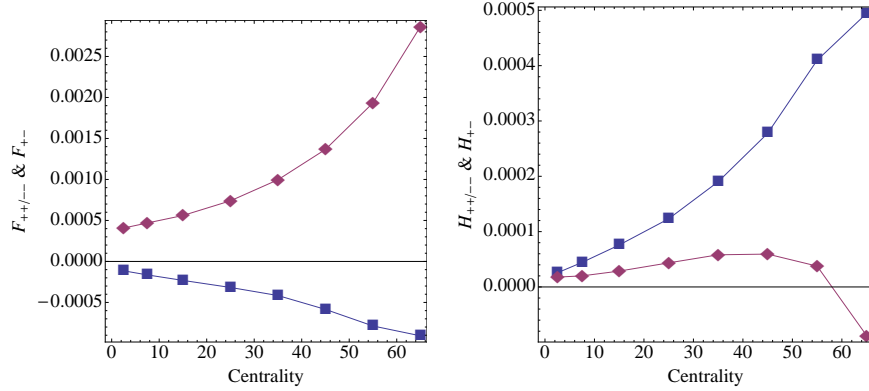


Fig. 11 The strength factors $F_{\alpha,\beta}$ (left) and $H_{\alpha,\beta}$ (right) extracted from the decomposition analysis (see text for details). The blue boxes and red diamonds are for $++/--$ and $+-$, respectively.

There is a strong residual centrality dependence for both types component, although the dependence on centrality from v_2 has been removed. This may indicate that the correlations depend also on the multiplicity, which changes from central to peripheral collisions.

Although, as already noted, the above analysis is qualitative, let us entertain a possible scenario, which would be consistent with the above observations: The flow-induced signals may have two sources, the TMC with $F_{++/--}^{TMC} = F_{+-}^{TMC} < 0$ and the LCC with $F_{++/--}^{LCC} = 0$ and $F_{+-}^{LCC} > |F_{+-}^{TMC}| > 0$. The flow-independent signals may be from two different sources, the CME with $H_{++/--}^{CME} > 0$ and $H_{+-}^{CME} < 0$ and the dipole asymmetry from fluctuations (DAF) with $H_{++/--}^{DAF} = H_{+-}^{DAF} > 0$. Such a combination would indeed lead to correlations with magnitude and sign in qualitative agreement with the data. However, a quantitative analysis would have to be based on the exact decomposition based on Eq. (44). Alternatively, one may attempt a separation of flow dependent and flow independent contributions in experiment. How this could be achieved will be discussed in the following.

4.6 Suppression of elliptic-flow-induced correlations

In this chapter we will discuss the possibility of removing the elliptic-flow-induced background from the experimental data.

As seen in Eq. (44) all contributions due to correlations are proportional to the elliptic flow parameter, v_2 . Therefore, it would be desirable to control or remove this contribution by a suitable measurement. There are essentially two ways to go about this.

First, as proposed in Ref. [53], is to study collisions of deformed nuclei, such as $U + U$. By selecting very central, “face on face” collisions where the deformation of the nuclei is imprinted on the fireball, elliptic flow should be generated while at the same time the magnetic field will be very small. Should one observe correlations of the same magnitude and structure as ones already reported by STAR, this would identify their origin as being due to conventional two-particle correlations. The observation of considerably smaller correlations combined with a sizable v_2 , on the other hand, would lend support for the existence of the CME. This approach, while challenging to analyze, is at present being attempted at RHIC, were first $U + U$ collisions were made available.

Alternatively, as proposed in Ref. [45] one may make use of the large event-by-event fluctuations of v_2 . By selecting events with different v_2 in a given centrality class we can control this background. In principle the measurement can be extrapolated to $v_2 = 0$ (and consequently $v_2(p_t, \eta) = 0$) which will allow to extract correlations that only depend on the reaction plane orientation. Indeed, as presented in Fig. 12 even at $b = 10$ fm we expect a large fluctuation of initial eccentricity that will translate to large fluctuations of elliptic flow v_2 .

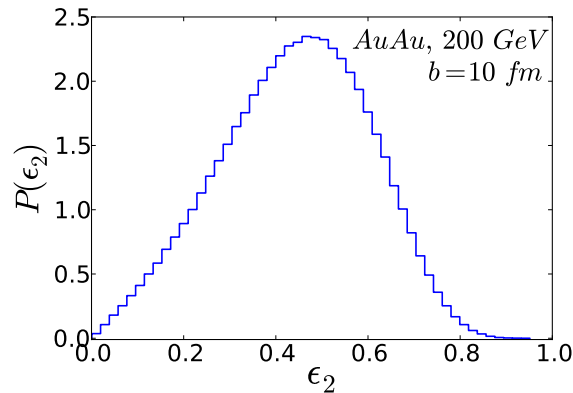


Fig. 12 The distribution of initial eccentricity ϵ_2 calculated in the Glauber Monte-Carlo at the impact parameter $b = 10$ fm.

Of course it is important to remove this background under the condition that the contribution from the Chiral Magnetic Effect is approximately unchanged. In Fig. 13 we demonstrate that indeed it is the case. Both the wounded nucleons and spectators’ contribution to the magnetic field weakly depends on ϵ_2 .

We believe this analysis should help to clarify the situation. Observation of non-zero γ_{++} or γ_{+-} at vanishing value of elliptic anisotropy v_2 will suggest

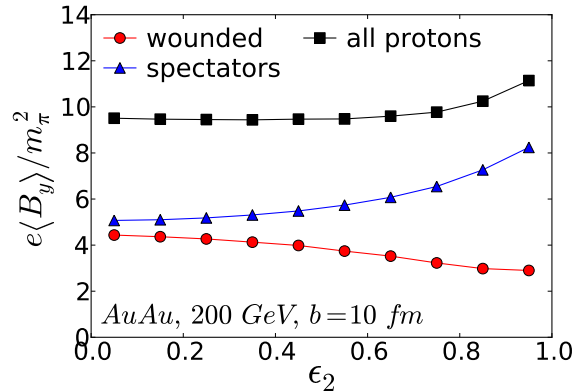


Fig. 13 The out-of-plane component of the magnetic field from wounded protons and spectator protons as a function of initial eccentricity ϵ_2 at a given impact parameter $b = 10$ fm.

the existence of the correlation mechanism that is sensitive to the average direction of the magnetic field – possibly the Chiral Magnetic Effect.

To summarize this Section, clearly there are many contributions based on conventional physics which contribute to the azimuthal correlations analyzed by the various experiments. In addition to those discussed in more detail in this Section other mechanisms, such as the decay of multi-particle clusters [36], have been proposed. While it is more difficult to assess their contribution quantitatively, their influence cannot a priori be ignored. Therefore, it seems the best way forward is to separate the influence of elliptic flow and magnetic field experimentally as discussed in the last part of this Section.

5 Summary and Conclusions

In this review we have concentrated on the observational aspects of the search for phenomena related to local parity violation of the strong interaction. Specifically we have discussed various observables and their measurement for the charge separation, which is a predicted consequence of induced currents due to sphaleron and anti-sphaleron transitions in an external magnetic field. This phenomenon is often referred to as the Chiral Magnetic Effect (CME).

We have discussed various properties and aspects of azimuthal angle correlations, and we have emphasized that, due to the elliptic flow observed in heavy ion collisions, virtually any two-particle correlations contribute to the azimuthal correlations. We have further discussed an alternative observable, which in our view may be better suited in discriminating between the backgrounds and the CME.

We have examined the presently available data on reaction plane dependent and independent correlation functions of same- and opposite-charged pairs. Our phenomenological analysis of the data by the STAR collaboration showed that the measured correlations of same-charge pairs are predominantly back-to-back, and in-plane. This is opposite to the predictions from the CME, where same-side out-of-plane correlations for pairs of the same charge are expected. The data by the ALICE collaboration taken at about ten times the STAR collision energy, on the other hand, show a correlation, albeit small, which is qualitatively consistent with the CME expectations.

However, before any conclusion on the CME can be drawn, the contributions due to “conventional” correlations need to be accounted for. As we have discussed in some detail, both the conservation of transverse momentum as well as local charge conservation give rise to corrections which are of the same order as the experimental signal. These need to be understood and properly subtracted from the data in order to see if a signal consistent with the CME remains. Since there are conceivably many other two-particle correlations, which may enter due to the presence of elliptic flow, an important step towards answering the question about the existence of the CME is to experimentally disentangle the elliptic flow phenomenon from the creation of a strong magnetic field. This can be either done by colliding deformed nuclei or by carefully utilizing the fluctuations of the elliptic flow.

In conclusion, the present experimental evidence for the existence of the CME is rather ambiguous. While progress on the assessment of the various background terms is to be expected, the sheer variety of possible correlations will likely limit a reliable quantitative determination of all the backgrounds. Therefore, the most important next step is the experimental separation of elliptic flow and magnetic field. In this context it is encouraging to note, that the first $U + U$ collisions at RHIC have just been recorded.

Finally let us close with a note of caution. Besides the CME there are other phenomena related to local non-vanishing topological charge fluctuations, such as the Chiral Magnetic Wave. One of the predictions in this case is the difference of elliptic flow between positively and negatively charged pions for collisions at lower energies [20]. However, again there may be other, more mundane effects which lead to similar phenomena, such as an increased stopping of baryon number and isospin at lower energies [54].

Acknowledgments

A. B. was supported by Contract No. DE-AC02-98CH10886 with the U. S. Department of Energy. V. K. was supported by the Office of Nuclear Physics in the US Department of Energy’s Office of Science under Contract No. DE-AC02-05CH11231. J. L. is grateful to the RIKEN BNL Research Center for partial support. A. B. also acknowledges the grant No. N202 125437 of the Polish Ministry of Science and Higher Education (2009-2012).

References

1. G. 't Hooft, arXiv:hep-th/0010225.
2. T. Schafer and E. V. Shuryak, Rev. Mod. Phys. **70**, 323 (1998).
3. E. Shuryak, “*The QCD Vacuum, Hadrons and Superdense Matter*”, 2nd ed., World Scientific Publishing Company, 2004.
4. G. Ripka, arXiv:hep-ph/0310102.
5. G. S. Bali, arXiv:hep-ph/9809351.
6. J. Greensite, Prog. Part. Nucl. Phys. **51**, 1 (2003).
7. J. Liao and E. Shuryak, Phys. Rev. C **75**, 054907 (2007); Phys. Rev. Lett. **101**, 162302 (2008). M. N. Chernodub and V. I. Zakharov, Phys. Rev. Lett. **98**, 082002 (2007). A. D’Alessandro and M. D’Elia, Nucl. Phys. B **799**, 241 (2008). M. Cristoforetti and E. Shuryak, Phys. Rev. D **80**, 054013 (2009). A. D’Alessandro, M. D’Elia and E. Shuryak, Phys. Rev. D **81**, 094501 (2010).
8. J. Liao and E. Shuryak, Phys. Rev. C **77**, 064905 (2008); Phys. Rev. D **73**, 014509 (2006); Nucl. Phys. A **775**, 224 (2006).
9. E. Shuryak, Prog. Part. Nucl. Phys. **62**, 48 (2009). D. E. Kharzeev, Nucl. Phys. A **827**, 118C (2009).
10. J. Liao and E. Shuryak, Phys. Rev. Lett. **102**, 202302 (2009). E. Shuryak, Phys. Rev. C **80**, 054908 (2009) [Erratum-ibid. C **80**, 069902 (2009)]. C. Ratti and E. Shuryak, Phys. Rev. D **80**, 034004 (2009). M. Lublinsky, C. Ratti and E. Shuryak, Phys. Rev. D **81**, 014008 (2010). D. M. Ostrovsky, G. W. Carter and E. V. Shuryak, Phys. Rev. D **66**, 036004 (2002).
11. D. Kharzeev, Phys. Lett. B **633**, 260 (2006).
12. D. Kharzeev and A. Zhitnitsky, Nucl. Phys. A **797**, 67 (2007).
13. D. E. Kharzeev, L. D. McLerran and H. J. Warringa, Nucl. Phys. A **803**, 227 (2008).
14. K. Fukushima, D. E. Kharzeev and H. J. Warringa, Phys. Rev. D **78**, 074033 (2008); Nucl. Phys. A **836**, 311 (2010). D. E. Kharzeev and H. J. Warringa, Phys. Rev. D **80**, 034028 (2009).
15. P. V. Buividovich, M. N. Chernodub, E. V. Luschevskaya and M. I. Polikarpov, Phys. Rev. D **80**, 054503 (2009). P. V. Buividovich, M. N. Chernodub, E. V. Luschevskaya and M. I. Polikarpov, Nucl. Phys. B **826**, 313 (2010).
16. D. E. Kharzeev, Annals Phys. **325**, 205 (2010).
17. D. T. Son and A. R. Zhitnitsky, Phys. Rev. D **70**, 074018 (2004) [arXiv:hep-ph/0405216].
18. M. A. Metlitski and A. R. Zhitnitsky, Phys. Rev. D **72**, 045011 (2005) [arXiv:hep-ph/0505072].
19. D. E. Kharzeev and H. -U. Yee, Phys. Rev. D **83**, 085007 (2011) [arXiv:1012.6026 [hep-th]].
20. Y. Burnier, D. E. Kharzeev, J. Liao and H. -U. Yee, Phys. Rev. Lett. **107**, 052303 (2011) [arXiv:1103.1307 [hep-ph]].
21. J. Rafelski and B. Muller, Phys. Rev. Lett. **36**, 517 (1976).
22. V. Skokov, A. Illarionov and V. Toneev, Int. J. Mod. Phys. A **24**, 5925 (2009)
23. A. Bzdak and V. Skokov, Phys. Lett. B **710**, 171 (2012) [arXiv:1111.1949 [hep-ph]].
24. W. -T. Deng and X. -G. Huang, Phys. Rev. C **85**, 044907 (2012) [arXiv:1201.5108 [nucl-th]].
25. B. Muller and A. Schafer, Phys. Rev. C **82**, 057902 (2010) [arXiv:1009.1053 [hep-ph]]. M. Asakawa, A. Majumder and B. Muller, Phys. Rev. C **81**, 064912 (2010) [arXiv:1003.2436 [hep-ph]].
26. V. D. Toneev, V. Voronyuk, E. L. Bratkovskaya, W. Cassing, V. P. Konchakovski and S. A. Voloshin, Phys. Rev. C **85**, 034910 (2012) [arXiv:1112.2595 [hep-ph]].

27. B. I. Abelev *et al.* [STAR Collaboration], Phys. Rev. Lett. **103**, 251601 (2009); Phys. Rev. C **81**, 054908 (2010).
28. S. A. Voloshin, Phys. Rev. C **70**, 057901 (2004).
29. J. Błoczynski, X. -G. Huang, X. Zhang, and J. Liao, in preparation.
30. S. A. Voloshin, A. M. Poskanzer and R. Snellings, arXiv:0809.2949 [nucl-ex].
31. S. Chatrchyan *et al.* [CMS Collaboration], JHEP **1107**, 076 (2011) [arXiv:1105.2438 [nucl-ex]]. G. Aad *et al.* [ATLAS Collaboration], arXiv:1203.3087 [hep-ex]. B. Abelev *et al.* [ALICE Collaboration], arXiv:1205.5761 [nucl-ex].
32. V. Koch, A. Majumder and J. Randrup, Phys. Rev. Lett. **95**, 182301 (2005) [nucl-th/0505052].
33. X. Zhang and J. Liao, Phys. Lett. B **713**, 35 (2012) [arXiv:1202.1047 [nucl-th]]. J. Liao, AIP Conf. Proc. **1441**, 874 (2012) [arXiv:1109.0271 [nucl-th]].
34. A. Bzdak, V. Koch and J. Liao, Phys. Rev. C **81**, 031901 (2010).
35. J. Liao, V. Koch and A. Bzdak, Phys. Rev. C **82**, 054902 (2010) [arXiv:1005.5380 [nucl-th]].
36. F. Wang, Phys. Rev. C **81**, 064902 (2010) [arXiv:0911.1482 [nucl-ex]]. Q. Wang, arXiv:1205.4638 [nucl-ex].
37. N. N. Ajitanand, R. A. Lacey, A. Taranenko and J. M. Alexander, Phys. Rev. C **83**, 011901 (2011) [arXiv:1009.5624 [nucl-ex]].
38. S. Schlichting and S. Pratt, Phys. Rev. C **83**, 014913 (2011)
39. B. Abelev *et al.* [ALICE Collaboration], arXiv:1207.0900 [nucl-ex].
40. V. D. Toneev and V. Voronyuk, Phys. Atom. Nucl. **75**, 607 (2012) [arXiv:1012.1508 [nucl-th]].
41. B. Mohanty [STAR Collaboration], J. Phys. G G **38**, 124023 (2011) [arXiv:1106.5902 [nucl-ex]].
42. S. Pratt, S. Schlichting and S. Gavin, Phys. Rev. C **84**, 024909 (2011)
43. A. Bzdak, V. Koch and J. Liao, Phys. Rev. C **83**, 014905 (2011)
44. G. -L. Ma and B. Zhang, Phys. Lett. B **700**, 39 (2011)
45. A. Bzdak, Phys. Rev. C **85**, 044919 (2012)
46. N. Borghini, P. M. Dinh and J. -Y. Ollitrault, Phys. Rev. C **62**, 034902 (2000)
47. S. Pratt, arXiv:1002.1758 [nucl-th].
48. Z. Chajecski and M. Lisa, Phys. Rev. C **78**, 064903 (2008)
49. A. Bialas, M. Bleszynski and W. Czyz, Nucl. Phys. B **111**, 461 (1976).
50. M. M. Aggarwal *et al.* [STAR Collaboration], Phys. Rev. C **82**, 024905 (2010)
51. P. Bozek and W. Broniowski, arXiv:1204.3580 [nucl-th].
52. D. Teaney and L. Yan, Phys. Rev. C **83**, 064904 (2011)
53. S. A. Voloshin, Phys. Rev. Lett. **105**, 172301 (2010)
54. J. Steinheimer, V. Koch and M. Bleicher, arXiv:1207.2791 [nucl-th].